EXTERNAL FIELD-INDUCED SQUEEZING IN A FOUR-LEVEL ATOM INSIDE A CAVITY SYSTEM

by

Eied Mahmoud KHALIL [a*], ***Mahmoud Y. ABD-RABBOU*** [b,c], ***Hammad ALOTAIBI*** [a], ***and Raed ALTHOBAITI*** [a]

[a] Department of Mathematics, College of Science, Taif University, Taif, Saudi Arabia
[b] Mathematics Department, Faculty of Science, Al-Azhar University, Nasr City, Cairo, Egypt
[c] School of Physics, University of Chinese Academy of Science, Beijing, China

Original scientific paper
https://doi.org/10.2298/TSCI2406855K

This paper delves into the influence of an external classical field on the statistical and dynamical properties of a four-level atom interacting with a cavity field. Leveraging mathematical transformations applied to the external classical field, the system's wave function was derived. Subsequently, the impact of this external field and a detuning parameter on atomic inversion, Shannon-entropy, the Q-function, and relative coherence is explored. The analysis encompassed three distinct initial states for the atomic system. The results unveiled that the specific type of classical field employed acts as a control parameter, inducing squeezing within the system, as demonstrably evidenced by the Q-function analysis. Conversely, the influence of the detuning parameter exhibited dependence on the initial state of the atomic system. However, in broader terms, it appears to be responsible for driving the system towards chaotic behavior.

Key words: *external classical field, shannon-entropy, Q-function, relative coherence.*

Introduction

Since quantum entanglement is thought to be the key idea that separates quantum information theory from classical theory, many researchers have been interested in studying it [1]. In quantum information, quantum computation, quantum cryptography, and teleportation, entanglement is essential [2-4]. A lot of work has gone into describing the characteristics of entanglement between quantum systems from the standpoints of applied and theoretical quantum information. Several methods for creating multiparticle entanglement have been put forth. The Jaynes-Cummings model (JCM) [5] is used to study the entanglement between the atom and the field. The JCM is still a key model in quantum optics even though it is straightforward in explaining how a two-level atom interacts with a single-mode quantum radiation field [6, 7]. Notably, the JCM has been nearly perfectly realized in tests using Rydberg atoms in superior superconducting cavities [7]. This model provides a theoretical foundation for forecasting a variety of fascinating events, such as atomic-field entanglement [7] and quantum collapse and revival [8]. There has also been a lot of interest in JCM generalizations to the two-atom state [9]. The impact of external fields on the dynamics of entanglement between a qubit and a single-mode field has been studied [9]. It has also been investigated how the Kerr medium, or Stark shift, affects the interaction of a multi-level atom in a cavity filled with a single-mode

* Corresponding author, e-mail: eiedkhalil@yahoo.com

field [10, 11]. On the other hand, research has been done on how an external field affects the interaction of two two-level atoms when there is a single- and two-mode field present [12, 13]. The impact of external classical fields on atom-field interactions has been the subject of recent research involving a variety of external environments, such as magnomechanical systems [14, 15], graphene layers [16, 17], and optomechanical cavities [18, 19].

Furthermore, analyzing statistical features and their connection the dynamical evolution of the system is an essential part of researching light-matter interactions [20]. Within this framework, atomic inversion, quasi-probability distributions, and information entropy become potent instruments that provide deep understanding of the dynamics and information that the quantum system contains. A crucial parameter for understanding and describing the behavior of atoms interacting with electromagnetic fields is atomic inversion, which is measured by the population difference between the ex-cited and ground states of the atom [21]. It supports a number of phenomena, such as the creation of non-classical light states [22], coherent control [23], and lasing [24]. A fundamental idea in information theory, Shannon-information entropy has found a home in the study of quantum systems [25]. It measures the amount of information or uncertainty connected to a specific quantum state [26]. Deciphering phenomena like entanglement, decoherence, and the dynamics of open quantum systems has been made possible by this idea [27, 28]. A high entropy value frequently indicates a mixed state of the system in the context of atom-field interactions [29]. Lastly, the Husimi Q-function and the Wigner function are examples of quasi-probability distributions that have become effective tools for examining and visualizing the phase-space representations of quantum states [30, 31]. Through the use of classical-like variables, these distributions allow for the interpretation of quantum phenomena, bridging the gap between the quantum and classical descriptions of physical systems [32]. The field subsystem [33], the atomic subsystem [34, 35], or even the atom and field simultaneously [36] can all be analyzed using quasi-probability distributions in the context of quantum systems.

Description of the physical model

This study examines a physical system consisting of a single diamond-shaped four-level atom surrounded by a cavity field and simultaneously stimulated by an external classical laser field. The ground state, represented by the symbol $|l_1\rangle$, and the two intermediate states, $|l_2\rangle$ and $|l_3\rangle$, are the permitted transitions between the atomic energy levels. Transitions from these intermediate states to the stimulated state, denoted by $|l_4\rangle$, are also permitted. A two-photon quantized field is the classical field. The system is described by the Hamiltonian operator ($\hbar = 1$):

$$\hat{H} = \hat{H}_{\text{free}} + \hat{H}_{\text{int}} + \hat{H}_{\text{ex}} \tag{1}$$

where

$$\begin{aligned} \hat{H}_{\text{free}} &= \omega_f \hat{a}^{\dagger}\hat{a} + \sum_{i=1}^{4} \omega_i \hat{\sigma}_{ii} \\ \hat{H}_{\text{int}} &= \lambda_1 \left[i \left(\hat{a}^{\dagger 2} - \hat{a}^2 \right) (\hat{\sigma}_{12} + \hat{\sigma}_{13} + \hat{\sigma}_{24} + \hat{\sigma}_{34}) + h.c. \right] \\ \hat{H}_{\text{ex}} &= \lambda_2 \left(\hat{a}^{\dagger 2} + \hat{a}^2 \right) \end{aligned} \tag{2}$$

where ω_f and ω_i are the characteristic frequencies of the cavity field and the atomic transition, respectively, λ_1 and λ_1 – the parameters quantify the coupling strengths between the atom and the cavity field, and the external field, respectively, $\hat{a}$ – the bosonic annihilation of the quantized field with the hermitian conjugate $\hat{a}^{\dagger}$ which satisfy $[\hat{a}, \hat{a}^{\dagger}] = I$, and $\sigma_{ij} = |l_i\rangle\langle l_j|$ represent the atomic flip operators.

To address the final term in the system's fundamental equation, eq. (1), we propose the canonical transformation:

$$\hat{a} = \hat{b}\cosh\zeta - \hat{b}^{\dagger}\sinh\zeta,\ \ \hat{a}^{\dagger} = \hat{b}^{\dagger}\cosh\zeta - \hat{b}\sinh\zeta \tag{3}$$

where

$$\zeta = \frac{1}{2}\tanh^{-1}\left(\frac{2\lambda_2}{\omega_f}\right)$$

and the operator $\hat{b}(\hat{b}^{\dagger})$ is annihilation (creation) operator and have the same meaning as the operators $\hat{a}(\hat{a}^{\dagger})$. Following this substitution of eq. (3) (which likely defines the transformed Hamiltonian using the displacement parameter) into the original Hamiltonian, eq. (1), the effect of the external classical field becomes effectively merged with the electromagnetic field within the Hamiltonian. Under the wave-rotating approximation, which simplifies the time-dependent terms in the Hamiltonian, the system transforms into a new form:

$$\hat{H} = \Omega_f \hat{b}^{\dagger}\hat{b} + \sum_{i=1}^{4}\omega_i\hat{\sigma}_{ii} + i\lambda_1(\hat{b}^{\dagger 2}(\hat{\sigma}_{12} + \hat{\sigma}_{13} + \hat{\sigma}_{24} + \hat{\sigma}_{34}) + h.c.) \tag{4}$$

where the new coupling of the free field takes

$$\Omega_f = \sqrt{\omega^2 - 4\lambda_2^2}$$

via applying the Heisenberg equation of motion, the physical Hamiltonian (1) can be written:

$$\hat{\mathcal{H}} = \Omega_f \mathcal{N} + \Omega_1 \mathcal{I} + \mathcal{H}_{\text{int}} \tag{5}$$

where

$$\mathcal{I} = \sum_{r=1}\hat{S}_{rr},\ \ \mathcal{N} = \hat{b}^{\dagger}\hat{b} - \hat{S}_{ii} - \hat{S}_{ff} - 2\hat{S}_{gg}$$

and the interaction Hamiltonian, $\mathcal{H}_{\text{int}}$, is obtained:

$$\mathcal{H}_{\text{int}} = \begin{bmatrix} 0 & -i\lambda_1\hat{b}^2 & -i\lambda_1\hat{b}^2 & 0 \\ i\lambda_1\hat{b}^{2\dagger} & \delta_1 & 0 & -i\lambda_1\hat{b}^2 \\ i\lambda_1\hat{b}^{2\dagger} & 0 & \delta_2 & -i\lambda_1\hat{b}^2 \\ 0 & i\lambda_1\hat{b}^{2\dagger} & i\lambda_1\hat{b}^{2\dagger} & \delta_3 \end{bmatrix} \tag{6}$$

where $\delta_1 = \Omega_f - \Delta_1$, $\delta_2 = \Omega_f - \Delta_2$, and $\delta_3 = 2\Omega_f - \Delta_3$, with $\Delta_1 = \omega_1 - \omega_2$, $\Delta_2 = \omega_1 - \omega_3$, and $\Delta_3 = \omega_1 - \omega_4$. Using the complete resonance condition ($\delta_1 + \delta_2 = 0$, $\delta_3 = 0$) we can obtain the time evolution operator $\hat{U}(t) = \exp(-i\hat{H}_{\text{int}}t)$:

$$\hat{U}(t) = \begin{bmatrix} 1+\hat{b}^{2\dagger}\hat{A}\hat{b}^2 & \frac{\delta}{2\lambda_1}\hat{b}^{2\dagger}\hat{A} - i\hat{b}^{2\dagger}\hat{B} & \frac{-\delta_1}{2\lambda_1}\hat{b}^{2\dagger}\hat{A} - i\hat{b}^{2\dagger}\hat{B} & \hat{b}^{2\dagger}\hat{A}\hat{b}^{2\dagger} \\ \frac{\delta_1}{2\lambda_1}\hat{A}\hat{b}^2 - i\hat{B}\hat{b}^2 & \frac{\hat{\mu}_1^2}{2\lambda_1^2}\hat{A} - \frac{i\delta_1}{\lambda_1}\hat{B} + 1 & \frac{\hat{b}^{2\dagger}\hat{b}^2 + \hat{b}^2\hat{b}^{2\dagger}}{2}\hat{A} & \frac{\delta_1}{2\lambda_1}\hat{A}\hat{b}^{2\dagger} - i\hat{B}\hat{b}^{2\dagger} \\ \frac{-\delta_1}{2\lambda_1}\hat{A}\hat{b}^2 - i\hat{B}\hat{b}^2 & \frac{\hat{b}^{2\dagger}\hat{b}^2 + \hat{b}^2\hat{b}^{2\dagger}}{2}\hat{A} & \frac{\hat{\mu}_1^2}{2\lambda_1^2}\hat{A} + \frac{i\delta}{\lambda_1}\hat{B} + 1 & \frac{-\delta_1}{2\lambda_1}\hat{A}\hat{b}^{2\dagger} - i\hat{B}\hat{b}^{2\dagger} \\ \hat{b}^2\hat{A}\hat{b}^2 & \frac{\delta_1}{2\lambda_1}\hat{b}^2\hat{A} - i\hat{b}^2\hat{B} & \frac{-\delta_1}{2\lambda_1}\hat{b}^2\hat{A} - i\hat{b}^2\hat{B} & 1+\hat{b}^2\hat{A}\hat{b}^{2\dagger} \end{bmatrix}$$

where

$$\hat{A} = \frac{2\lambda_1^2(\cos^2\hat{\mu}_2 t - 1)}{\hat{\mu}_2^2},\ \hat{B} = \frac{\lambda_1 \sin\hat{\mu}_2 t}{\hat{\mu}_2}$$

$$\hat{\mu}_2^2 = \delta_1^2 + 2\lambda_1^2(\hat{b}^{2\dagger}\hat{b}^2 + \hat{b}^2\hat{b}^{2\dagger}),\ \hat{\mu}_1^2 = \delta_1^2 + \lambda_1^2(\hat{b}^{2\dagger}\hat{b}^2 + \hat{b}^2\hat{b}^{2\dagger})$$

The method of computation now necessitates the determination of appropriate initial conditions for the operator $\hat{b}$. Since the problem commenced with the operator $\hat{a}$ and transitioned to $\hat{b}$ through a canonical transformation, we leverage the established relationship between them to ascertain a suitable initial state for the system. As observed, the coherent state $|\mathcal{Z}\rangle$ represents the initial state corresponding to the new operator $\hat{b}$. However, it is crucial to establish the connection between this state and the physical operator $\hat{a}$pertaining to the initial coherent state, denoted by $|\alpha\rangle = \exp(\alpha\hat{a}^\dagger - \alpha^*\hat{a})|0\rangle$ (where $|0\rangle$ represents the vacuum state). In this context, we aim to identify the relationship between these two coherent states. Utilizing eq. (3) (which likely defines the transformed operator), a straightforward derivation yields:

$$\mathcal{Z} = \alpha\cosh\zeta + \alpha^*\sinh\zeta \tag{7}$$

where the operator $\hat{a}$'s eigenvalue with regard to the coherent state $|\alpha\rangle$ is α. This equation shows that, in comparison the initial coherent state $|\alpha\rangle$ for the original operator $\hat{a}$, the coherent state $|\mathcal{Z}\rangle$ for the modified operator $\hat{b}$ corresponds to a compressed coherent state. The previously defined displacement parameter ζ determines the squeezing parameter. After some computations, we discover:

$$|\mathcal{Z}\rangle = \sum_{n=0}^{\infty} Q_n |n\rangle,\ Q_n = \frac{\exp\left(\frac{-|\beta|^2 + \beta^2\tanh\zeta}{2}\right)}{\sqrt{2^n n!\cosh\left(\frac{\beta}{\sqrt{\sinh 2\zeta}}\right)}}(\tanh\zeta)^{n/2} H_n\left(\frac{\beta}{\sqrt{\sinh 2\zeta}}\right) \tag{8}$$

where $H_n(z)$ is the Hermite polynomial of order n. For real α, we note that $\beta = \alpha\exp(\zeta)$ and it increases by increasing the parameter λ_2 as can be seen from the definition of ζ.

However, the initial atomic state is regulated in superpositio state:

$$|\psi_a(0)\rangle = \sum_{i=1}^{4} c_i |l_i\rangle,\ \text{where}\ \sum_{i=1}^{4}|c_i|^2 = 1 \tag{9}$$

Thus, through our discussion, the initial wave-vector of the field is in a squeezed state $|\mathcal{Z}\rangle$, while the atomic state exhibits one of the following three scenarios. In the first scenario, we consider the atomic system to be in the ex-cited state $|l_4\rangle$. Consequently, the initial state of the atom-field system:

$$|\psi_1(0)\rangle = |l_4\rangle \otimes |\mathcal{Z}\rangle$$

In the second scenario, the initial atomic state is in a superposition state

$$\frac{1}{\sqrt{2}}(|l_1\rangle + l_4\rangle)$$

Hence, the initial state of the total system in this case:

$$|\psi_2(0)\rangle = \frac{1}{\sqrt{2}}(|l_1\rangle + |l_4\rangle) \otimes |\mathcal{Z}\rangle$$

In the third scenario, the atomic system is in a superposition state:

$$\frac{1}{\sqrt{3}}\left(\left|l_4\right\rangle+\left|l_3\right\rangle+\left|l_2\right\rangle\right)$$

Therefore the initial state in this case:

$$|\psi_3(0)\rangle=\frac{1}{\sqrt{3}}(|l_4\rangle+|l_3\rangle+|l_2\rangle)\otimes|\mathcal{Z}\rangle$$

The temporal wave-vector of the system using the initial states (8) and (9), and the evolution operator $\hat{U}(t)$ (2) can be written:

$$\left|\psi(t)\right\rangle_{A-F}=\hat{U}(t)\otimes\left|\psi_a\right\rangle\otimes\left|\mathcal{Z}\right\rangle \tag{10}$$

Tracing out the field will yield the reduced density operator of the atomic system, and tracing out the atomic system will yield the reduced density operator of the field system. The operator for lower density is provided:

$$\hat{\rho}_{A(F)}(t)=Tr_{F(A)}\left[|\psi(t)\rangle_{A-F}\ {}_{A-F}\langle\psi(t)|\right] \tag{11}$$

Hereinafter, we will employ the temporal wave-vector (10) to discuss the evolution of atomic inversion, Shannon-information entropy and relative entropy of coherence. Moreover, we will investigate the phase space of the field subsystem by utilizing the Husimi Q-function. Through our discussion, we will assume that the intensity of coherent state $\alpha = 5$, and $\Delta_1 = \Delta_2 = \Delta_3 = \Delta$.

Atomic inversion and Shannon-entropy

This section discusses the effect of external field on the atomic population inversion and its relation with Shannon-information entropy. For the population inversion, we will use the reduced density operator of the atomic system $\hat{\rho}_A(t)$. The population inversion gives the general behaviour about the collapse and revival phenomenon of the atom field interaction. It is expressed for our system:

$$W(t)=e_{11}+e_{33}-(e_{22}+e_{44}) \tag{12}$$

where $e_i = {}_{A-F}\langle\psi(t)|\sigma_{ii}|\psi(t)\rangle_{A-F}$.

On the other hand, in the context of synthesizing probability distributions, Shannon-information is introduced as a concept aimed at addressing the efficient coding of a set of quantum states. It provides a framework within the domain of probability distribution quantify the amount of information carried by a signal or a set of quantum states. Shannon-entropy is defined [28]:

$$S_H(t)=-\frac{1}{\ln|\alpha|^2}\sum_{n=1}^{\infty}\mathcal{P}(t)\ln\mathcal{P}(t) \tag{13}$$

where $\mathcal{P}(t) = \langle n|\hat{\rho}_F(t)|n\rangle$, and α is the intensity of initial state.

Figure 1 depicts the temporal evolution of both atomic population inversion and Shannon-entropy under the influence of the classical field and detuning. The red curve represents the population inversion, while the blue curve corresponds to Shannon-entropy.

First row: The atomic system is initially prepared in an ex-cited state $|\psi_1\rangle$ with varying values of Δ, λ_2. In fig. 1(a) ($\Delta = 0$, $\lambda_2 \simeq 0$), the system exhibits well-defined periodic revivals and collapses with a period of $\lambda_2 t = 2n\pi$, $n = 0, 1, 2, \ldots$. This phenomenon arises due to the inherent periodicity of the atom-field interaction, leading to a periodic rephasing of the quantum states.

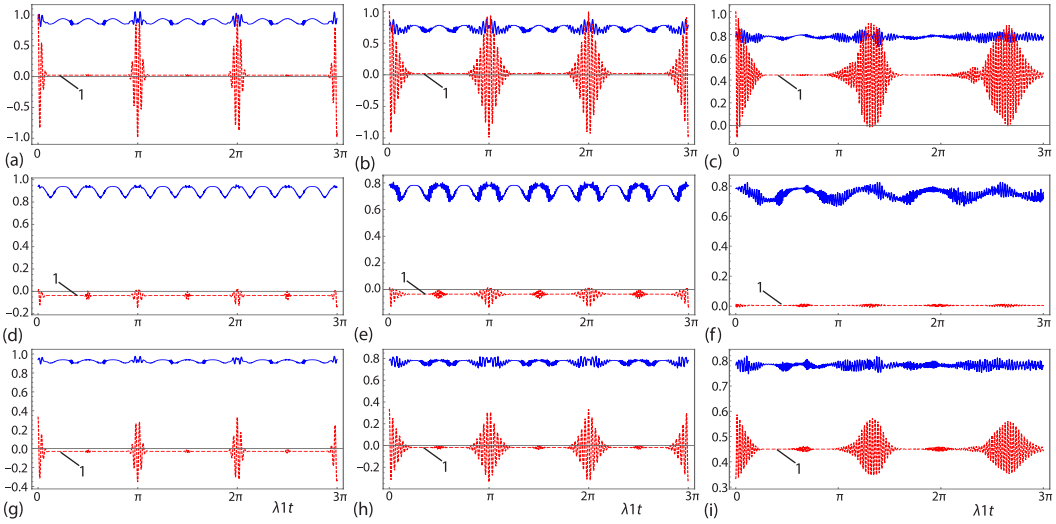

Figure 1. The evolution of atomic inversion curve – 1 and information Shannon-entropy as a function of scaled time $\lambda_1 t$ with $\alpha = 5$; the upper row: $|\psi(0)\rangle = |\psi_1\rangle$; (a) $\Delta = 0$, $\lambda_1 \simeq 0$, (b) $\Delta = 0$, $\lambda_2 = 0.49$, and (c) $\Delta = 50$, $\lambda_2 = 0.49$; the middle row is the same as the upper row but $|\psi(0)\rangle = |\psi_2\rangle$; the lower row is the same as the upper row but $|\psi(0)\rangle = |\psi_3\rangle$

Notably, despite the presence of collapse, the population inversion does not reach zero. This indicates the persistence of coherence or the possible achievement of a stable superposition state. However, the population inversion approaches zero as time progresses, demonstrating behavior similar to the two-photon Jaynes-Cummings model [13]. Furthermore, Shannon-entropy exhibits periodic oscillations around unity, suggesting that the system retains sufficient information for self-description, indicating a mixed state. As depicted in fig. 1(b), increasing $\lambda_2 = 0.49$ leads to a significant increase in the revival period. This signifies an enhanced rate of transitions between energy levels while maintaining the same periodicity observed in fig. 1(a). Conversely, Shannon-entropy decreases with increasing λ_2, but exhibits a more pronounced oscillatory behavior. The inclusion of $\Delta = 50$ and classical field $\lambda_2 = 0.4$, as shown in fig. 1(c), results in a positive atomic population inversion, indicating an approach towards the ex-cited state of the atomic system. The population inversion oscillations almost display the Jaynes-Cummings model's behaviour. Interestingly, Shannon-entropy exhibits a decrease with increasing Δ, accompanied by an increase in the amplitude and randomness of its oscillations.

Second row in fig. 1: Assuming the initial state of the atomic system is $|\psi_2\rangle$, we observe a general tendency for $W(t)$ to converge towards the zero line or even completely coincide with it, depending on the specific values of the external classical field and detuning parameter. In the absence of detuning (resonance condition), $W(t)$ exhibits a convergence towards zero irrespective of the presence or absence of the external field. Notably, the revival periods are significantly shorter compared to the case with an initial state of $|\psi_1\rangle$. This phenomenon can be attributed to the superposition state occupied by the atom, residing simultaneously in both the ex-cited and ground states, resulting in a minimal population inversion. Additionally, Shannon-entropy demonstrates periodic fluctuations around unity, signifying a persistent state of high information content (chaos) that necessitates coherence for interpretation. However, under detuning conditions (non-resonance), $W(t)$ coincides with the zero line during collapse periods, while revival periods exhibit markedly diminished amplitudes. Furthermore, $S_H(t)$ dis-

plays erratic and irregular oscillations, with maximum values lower than those observed under resonance conditions.

Third row in fig. 1: The behaviour of the atomic system is explored when the initial state is $|\psi_3\rangle$. The revival and collapse periods are similar to the case of $|\psi_1\rangle$ under resonance conditions, albeit with a reduction in oscillation amplitudes. Intriguingly, the collapse periods exhibit negative values. Interestingly, the behaviour of Shannon-entropy closely mirrors that of an initially ex-cited atomic state, suggesting that the information encoded within the system remains preserved despite variations in atomic population amplitudes. In the non-resonance case, the atomic population becomes entirely positive, exhibiting characteristics reminiscent of three-level systems under non-resonance conditions [37].

Husimi Q-function

The importance of the Husimi Q-function in quantum information theory and quantum optics is widely recognized. It is defined as the coherent expectation value of the reduced field density matrix and depicts the quasi-probability distribution of a quantum state in phase space. Thus, we may quantify and characterize squeezing phenomena in quantum systems by using the width of the Q-function as a quantitative measure of squeezing. The Q-function is provided mathematically [33]:

$$\mathcal{Q}(\beta,t)=\frac{1}{\pi}\left\langle \beta\left|\hat{\rho}_F(t)\right|\beta\right\rangle \tag{14}$$

Figure 2 explores the influence of the initial atomic state ($|\psi_1\rangle$, $|\psi_2\rangle$, $|\psi_1\rangle$), the classical field, λ_2, and detuning, Δ, on the system's phase space representation, denoted by the Q-function, within the complex β -plane, where $\beta = x + iy$. We focus on a specific time point ($\lambda_1 t = 1$) corresponding to the first collapse period of the atomic inversion. The decision exclude the time dependence is motivated by exploring this aspect in prior studies, particularly under conditions without an external classical field [38].

In the case of $|\psi_1\rangle$, figs. 2(a)-2(c): in the absence of both λ_2 and Δ, fig. 2(a), the Q-function exhibits three concentric circular peaks. The central peak, located at (0, 5), reflects the intensity parameter of the initial state α. The two smaller, flanking peaks, positioned approximately a (–2, ±4, 5), demonstrate sensitivity to changes in system parameters. As λ_2 increases , fig. 2(b), a squeezing effect is observed for all three peaks, transforming the concentric circles into ellipses. This phenomenon signifies that the classical field acts as a squeezing parameter, with a more pronounced effect observed at higher λ_2 values. Introducing detuning, Δ, fig. 2(c), leads to a reduction in the intensity and a shift in the positions of the secondary peaks within the β-plane.

In the case of $|\psi_2\rangle$, figs. 2(d)-2(f): fig. 2(d) depicts two main peaks forming concentric circles centered at(–2, ±4, 5) for the initial state $|\psi_2\rangle$. With increasing λ_2, fig. 2(e), these peaks undergo squeezing, transforming into ellipses while maintaining their central position. However, the introduction of Δ, fig. 2(f), results in the reappearance of the main peak observed for $|\psi_1\rangle$. This suggests that detuning enhances the phase when the atomic system is prepared in a superposition state.

In the case ofv $|\psi_3\rangle$, figs. 2(g)-2(i): in the absence of λ_2 and Δ, fig. 2(g), three peaks are observed for the initial state $|\psi_3\rangle$. However, the primary peak is approximately located at (–2, ±4, 5), with the other two peaks being considerably smaller. Figure 2(h) demonstrate that increasing the classical field, λ_2, leads to the squeezing of these initially circular peaks. Furthermore, introducing detuning, fig. 2(i), increases the number of contours within the Q-function representation and shifts the main peak to a position consistent with figs. 2(c) and 2(f).

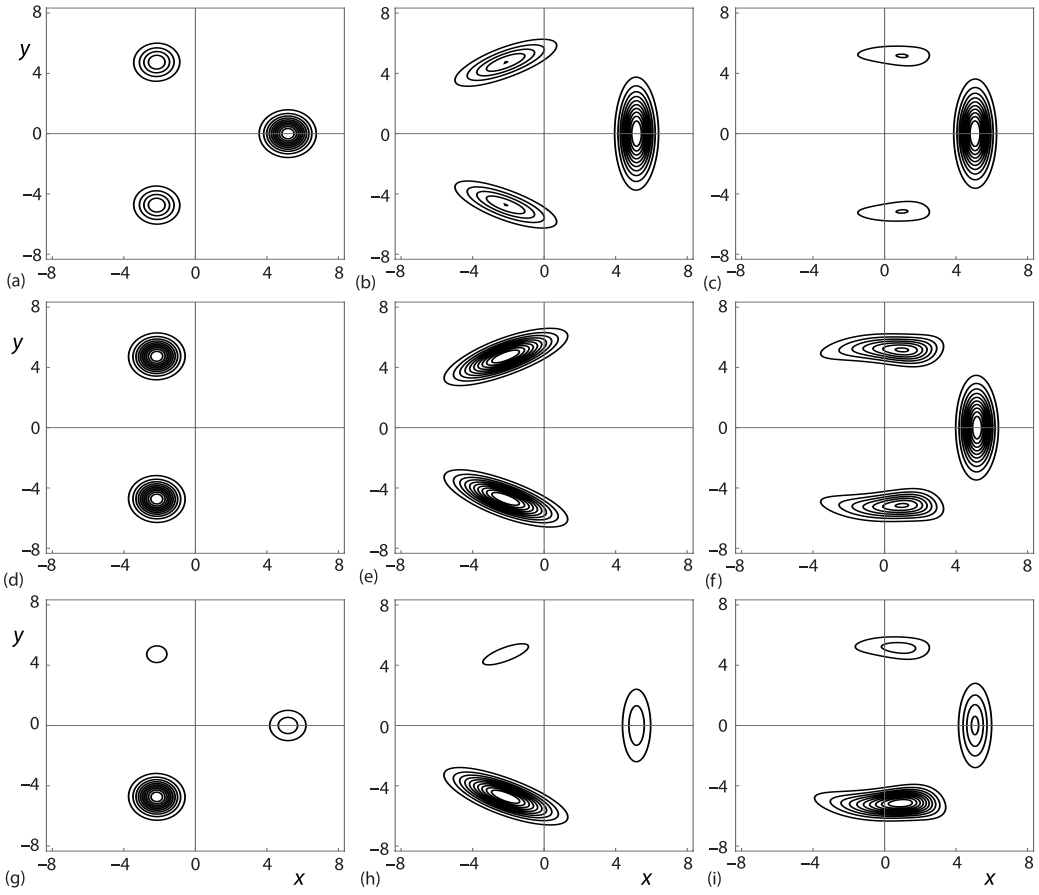

Figure 2. The contour plot of the Husimi Q-function in the complex plan $\beta = x + iy$ with the same parameters as fig. 1 and $\lambda_1 t = 1$

Relative entropy of coherence

To quantify the coherence of a quantum state relative to a known state, one can examine the relative entropy of coherence. In general, the coherence refers to superposition of quantum states. We will employ this measure to quantify the distinguishability between the temporal evolution of the atom quantum state $\hat{\rho}_A$ and the closest diagonal state diag($\hat{\rho}_A$) in terms of entropy. The relative entropy of coherence $\mathcal{C}(t)$ of the quantum state $\hat{\rho}_A$ with respect to a reference state diag($\hat{\rho}_A$) is defined [39]:

$$\mathcal{C}(t) = S\left[\text{diag}(\hat{\rho}_A)\right] - S(\hat{\rho}_A) = \sum_{i=1}^{4} \eta_i \ln \eta_i - \sum_{i=1}^{4} e_{ii} \ln e_{ii} \tag{15}$$

where η_i are the eigenvalues of the quantum state $\hat{\rho}_A$.

In fig. 3, we will discuss the effect of the initial state of the atomic system, the classical field, and detuning on the relative coherence $\mathcal{C}$ under the same conditions as in fig. 1.

For $|\psi_1\rangle$, figs. 3(a)-3(c): the $\mathcal{C}$ function exhibits a characteristic evolution. Starting at zero, signifying the initial absence of coherence, it undergoes a rapid rise to a value approach-

ing the maximum attainable value ($\mathcal{C} \simeq 1.3$). It is important to note that the theoretical maximum coherence for a four-level atom is $\mathcal{C} = 1.38$. Subsequently, the $\mathcal{C}$ function displays a pattern of semi-periodic oscillations. Large oscillations occur at specific time intervals ($\lambda_1 t = n\pi$, $n = 0, 1, 2, 3,...$) while smaller, damped oscillations appear at intermediate intervals ($\lambda_1 t = (n + 1)\pi/2$). Notably, the $\mathcal{C}$ function approaches a state of minimal coherence at these latter time points. Increasing λ_2 amplifies the coherence oscillations while maintaining their periodicity. However, introducing Δ leads to further amplification of the oscillations, albeit with a distinct change in their shape. These oscillations appear more random in nature. Despite these fluctuations, the overall coherence remains consistent with the phenomenon of atomic inversion.

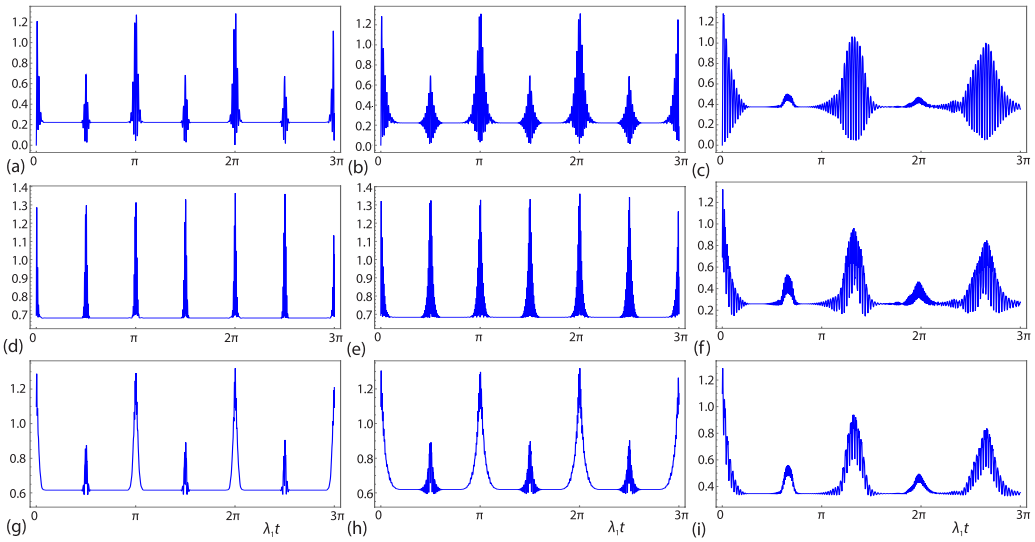

Figure 3. The dynamical behaviour of relative entropy of coherence $\mathcal{C}(t)$ with the same parameters as fig. 1

For $|\psi_2\rangle$, figs. 3(d)-3(f): in the absence of both λ_2 and Δ, fig. 3(d), the $\mathcal{C}$ function exhibits periodic oscillations at time intervals of $\lambda_1 t = n\pi/2$ for the initial state $|\psi_2\rangle$. Notably, the minimum value of coherence ($\mathcal{C} \simeq 0.7$) represents an improvement in relative coherence compared to $|\psi_1\rangle$. Furthermore, increasing scaled time leads to an enhancement of the maximum coherence values, reaching the theoretical limit ($\mathcal{C} = 1.38$) at the repetition periods. Similar to $|\psi_1\rangle$, increasing λ_2 amplifies the oscillations. However, the addition of Δ presents a contrasting effect. While coherence is amplified overall, the minimum value can reach as low as $\mathcal{C} = 0.2$ at certain time points. The relative coherence behavior for the initial state $|\psi_3\rangle$, figs. 3(g)-3(i), resembles the case of $|\psi_1\rangle$, figs. 3(a)-3(c), with some key distinctions. The minimum value of $\mathcal{C}$ is slightly higher ($\mathcal{C} \simeq 0.6$) for $|\psi_3\rangle$. Additionally, the $\mathcal{C}$ function does not start from zero due to the initial superposition state of the atom in this case.

Conclusions

This paper has explored the intricate interplay between a diamond configuration four-level atom and a cavity field under the influence of an external classical field. The study has examined the collective impact of the initial atomic state, detuning parameter, and external classical field on four key characteristics: atomic inversion, quantum Shannon-entropy, Q-function, and relative entropy of coherence.

The findings demonstrate a profound influence of the initial atomic state on both atomic inversion and Shannon-entropy patterns. Introducing the detuning parameter significantly enhanced the observed atomic inversion, particularly for measured or superposition initial states, driving the system closer to the ex-cited state. However, detuning also resulted in a reduction in the maximum achievable values of Shannon-entropy. The presence of an external classical field further amplified the oscillations observed in both atomic inversion and information entropy.

With regards to the Q-function, the initial atomic state was revealed to exert a significant influence on its behavior. The phase space for the measured state was demonstrably larger compared to that observed for the superposition initial state. The application of an external classical field resulted in the squeezing of the Q-function, with the classical field parameter acting as a squeezing factor. This confirms the transformation of the initial coherent state into a squeezed coherent state under the influence of this specific type of classical field. Conversely, the introduction of the detuning parameter led to a transformation in the Q-function's shape, with an observed increase in the phase space distribution.

Finally, the investigation into the relative entropy of coherence revealed a crucial role played by the initial atomic state in either increasing or decreasing its value. The coherence of the lower initial measured state was demonstrably lower compared to that observed for the initial superposition state. The external classical field also induced a rise in the lower values of the relative entropy of coherence. Detuning, however, contributed to an increase in the chaotic behavior within the system, leading to a reduction in the maximum achievable values of relative entropy of coherence.

Acknowledgments

The authors extend their appreciation to Taif University, Saudi Arabia, for supporting this work through project number (TU-DSPP-2024-71).

References

[1] Mendonca, J., *et al*., Generation and Distribution of Atomic Entanglement in Coupled-Cavity Arrays, *Phys. Rev. A*, *102* (2020), 6, 062416
[2] Gisin, N., *et al*., Rev. Mod. Phys., *Rev. Mod. Phys*., *74* (2002), 1, 145
[3] Bennett, C. H., Wiesner, S. J., Communication via one- and two- particle operators on Einstein-Bodolsky-Rosen States, *Phys. Rev. Lett*., *69* (1992), 20, 2881
[4] Abd-Rabbou, M. Y., Probing Teleported Quantum Correlations in a Two-Qubit System Inside a Coherent field, *Optik*, *296* (2024), 171551
[5] Jaynes, E. T., Cummings, F. W., Comparison of Quantum And Semiclassical Radiation Theories with Application the Beam Maser, *Proceedings of the IEEE*, *51* (1963), 1, pp. 89-109
[6] Shore, B., aKnight, P., The Jaynes-Cummings Model, *J. Mod. Opt*., *40* (1993), 7, pp. 1195-1238
[7] Walther, H., *et al.*, Cavity Quantum Electrodynamics, *Rep. Prog. Phys*., *69* (2006), 5, 1325
[8] Narozhny, N., *et al*., Coherence *vs*. Incoherence: Collapse and Revival in a Simple Quantum Model, *Phys. Rev. A*, 23 (1981), 1, 236
[9] Abdalla, M. S., *et al.*, Exact Treatment of the Jaynes-Cummings Model under the Action of an External Classical Field, *Ann. Phys*., *326* (2011), 9, pp. 2486-2498
[10] Obada, A.-S. F., *et al*., Generation of a Non-Linear Two-Mode Stark Shift Through the Adiabatic Elimination Method, *J. Mod. Optics*, *53* (2006), 08, pp. 1149-1163
[11] Obada, A. S.-F., *et al*., Entangled Two Two-Level Atoms Interacting with a Cavity Field in the Presence of the Stark Shift Terms, *Opt. Commun.*, *287* (2013), Jan., pp. 215-223
[12] Khalil, E., *et al.*, Pair Entanglement of Two-Level Atoms in the Presence of a Non-Degenerate Parametric Amplifier, *J. Phys. B*, *43* (2010), 9, 095507
[13] Obada, A.-S. F., *et al*., Influence of an External Classical Field on the Interaction Between a Field and an Atom in Presence of Intrinsic Damping, *Int. J. Theore. Phys*., *57* (2018), June, pp. 2787-2801

[14] Guo, Q., *et al*., Magnon-Squeezing by Two-Tone Driving of a Qubit in Cavity-Magnon-Qubit Systems, *Phys. Rev. A*, *108* (2023), 063703
[15] Alotaibi, M. F., *et al*., The Classicality and Quantumness of the Driven Qubit-Photon-Magnon-System, *Mathematics*, *10* (2022), 23, 4458
[16] Alruqi, A. B., *et al*., Visualization of the Interaction Dynamics between a Two-Level Atom and a Graphene Sheet Covered by a Laser Field, *Alex. Eng. J*., *77* (2023), Aug., pp. 309-317
[17] Alruqi, A. B., *et al*., Entanglement of a Cavity with a Three-Level Atom and a Graphene Membrane in the Presence of a Laser Field, *Alex. Eng. J*., *75* (2023), July, pp. 419-428
[18] Alotaibi, M. F., *et al*., Dynamics of an Atomic System Associated with a Cavity-Optomechanical System, *Res. Phys*., *37* (2022), 105540
[19] Foroughi, H., Daneshfar, N., Study of Optical Bistability in a Double-Cavity Hybrid Optomechanical System Consisting of an Optical Cavity Coupled with a Mechanical Resonator Filled with Semiconductor Quantum Dot Molecules, *Europ. Phys. J. D*, *77* (2023), 6, 118
[20] Gerry, C. C., Knight, P. L., *Introductory Quantum Optics*, Cambridge University Press, Cambridge, UK, 2023
[21] Scully, M. O., Zubairy, M. S., *Quantum Optics*, Cambridge University Press, Cambridge, UK, 1997
[22] Loredo, J., *et al*., Generation of Non-Classical Light in a Photon-Number Superposition, Nature Photonics, *13* (2019), 11, pp. 803-808
[23] Moon, H., *et al*., Coherence Control Using the Ratio of Rabi Frequencies for Complete Coherent Inversion in a Four-Level λ System, *J. Phys. B*, *32* (1999), 4, 987
[24] Scully, M. O., *et al*., Degenerate Quantum-Beat Laser: Lasing Without Inversion and Inversion Without Lasing, *Phys. Rev. Lett.*, *62* (1989), 24, 2813
[25] Shannon, C. E., *The Mathematical Theory of Communication*, University of Illinois Press, Champaign, Ill. USA, 1949
[26] Obada, A. S., *et al.*, Does Conditional Entropy Squeezing Indicate Normalized Entropic Uncertainty Relation Steering, *Quantum Inf. Process.*, *23* (2024), 3, 90
[27] Abdel-Aty, M., Quantum Information Entropy and Multi-Qubit Entanglement, *Prog. Quantum Electron*, *31* (2007), 1, pp.1-49
[28] Obada, A.-S. F., *et al*., Moving Three-Level λ-Type Atom in a Dissipative Cavity, *Europ. Phys. J. D*, *71* (2017), 338
[29] Adesso, G., *et al.*, Entanglement, Purity, and Information Entropies in Continuous Variable Systems, *Open Sys. and Inf. Dynam*., *12* (2005), 2, pp. 189-205
[30] Wigner, E., On the Quantum Correction for Thermodynamic Equilibrium, *Phys. Rev*., *40* (1932), June, pp. 749-759
[31] Husimi, K., Some Formal Properties of the Density Matrix, Proceedings of the Physico-Mathematical Society of Japan, *3rd Series*, 22 (1940), 4, pp. 264-314
[32] Lee, H.-W., Theory and Application of the Quantum Phase-Space Distribution Functions, *Physics Reports*, *259* (1995), 3, pp. 147-211
[33] Moya-Cessa, H., Knight, P. L., Series Representation of Quantum-Field Quasiprobabilities, *Phys. Rev. A*, *48* (1993), Sept., pp. 2479-2481
[34] Abd-Rabbou, M. Y., *et al*., Wigner Distribution of Accelerated Tripartite W-State, *Optik*, *208* (2020), 163921
[35] Abd-Rabbou, M. Y., *et al*., Non-Classical Correlations of Accelerated Observers Interacting with a Classical Stochastic Noise Beyond the Single Mode Approximation, *Opt. Quantum Electron*, *55* (2023), 8, 715
[36] Rundle, R. P., Everitt, M. J., Overview of the Phase Space Formulation of Quantum Mechanics with Application Quantum Technologies, *Adv. Quantum Techno*., *4* (2021), 6, 2100016
[37] Abdel-Aty, M., Quantum Phase Entropy and Entanglement of a Multiphoton Three-Level Atom Near the Edge of a Photonic Band Gap, *Laser Phys*., *16* (2006), Oct., pp. 1381-1394
[38] Abdel-Wahab, N., A Four-Level Atom Interacting with a Single-Mode Cavity Field: Double ξ-Configuration. *Modern Physics Letters B*, *22* (2008), 26, pp. 2587-2599
[39] Baumgratz, T., *et al*., Quantifying Coherence, *Phys. Rev. Lett.*, *113* (2014), 140401

Paper submitted: June 22, 2024
Paper revised: September 2, 2024
Paper accepted: October 21, 2024
2024 Published by the Vinča Institute of Nuclear Sciences, Belgrade, Serbia.
This is an open access article distributed under the CC BY-NC-ND 4.0 terms and conditions.